JOURNAL OF MATERIALS SCIENCE **34** (1999) 2921–2928

Fabrication of spherical magnetite particles by the flame fusion method

SHINICHI MIYAKE
Nippon Sanso Corporation, Technical Division, Yamanashi Laboratory, 3054-3, Shimokurosawa, Takane-cho, Kitakoma-gun, Yamanashi, 408-0015 Japan

NOBUKAZU KINOMURA
Institute of Inorganic Synthesis, Faculty of Engineering, Yamanashi University, 7, Miyamae-cho, Kofu-shi, Yamanashi, 400-8511 Japan

TAKASHI SUZUKI
Department of Applied Chemistry and Biotechnology, Faculty of Engineering, Yamanashi University, 4-3-11, Takeda, Kofu-shi, Yamanashi, 400-8511 Japan

TOSHIO SUWA
Nippon Sanso Corporation, Technical Division, Yamanashi Laboratory, 3054-3, Shimokurosawa, Takane-cho, Kitakoma-gun, Yamanashi, 408-0015 Japan

Fabrication of spherical magnetite powders was investigated in the propane-oxygen flame using sponge iron powders as a starting powder. Spherical particles produced by fusion, sphering and oxidation of iron powder were composed of residual Fe, FeO, Fe_3O_4 and α-Fe_2O_3 in the case of particles collected by a cyclone. The amount of Fe_3O_4 in the products was strongly dependent on the propane/oxygen ration and the flow rate of carrier air, but weakly on the feed rate of iron powder. Injection of quenching gas was found to be effective to improve the yield of Fe_3O_4. Particle size of products reflected directly that of starting powders, indicating fairly easy control of particle size of products. The saturation magnetization of the produced powder under the optimum condition was 88 emu/g. These facts suggest that the fusion and oxidation treatment of iron powders in the propane-oxygen flame is a suitable process for the manufacture of the magnetic carrier for plain paper copy (PPC) on an industrial scale. Powders collected by a bag filter were found to be fine γ-Fe_2O_3 particles with a diameter of about 100 nm.

1. Introduction

Spherical magnetite particles with diameter of several tens μm are considered to be a suitable material as a magnetic carrier for plain paper copy (PPC) due to their magnetic properties and low density and high fluidity [1], and have been investigated extensively [2]. Processes via solution phases are currently used for the fabrication of spherical magnetite particles. For example, fine spherical magnetite particles have been precipitated from ferrous solutions. However, particle size of spherical magnetite prepared from the solution was about 0.2 μm in diameter [3], and the powder is suitable for the single component toner development system, but not for the magnetic carrier for PPC. In addition, as the wet processes are complex, it is difficult to control the particle size as designed.

We have reported the fabrication of spherical silica used as a semiconductor encapsulating material by fusing ground natural quartz powders in the propane-oxygen flame [4, 5]. Remarkable features of this method are following; the particle size distribution of starting powders is almost maintained after the fusion, spherical particles are obtained with ease and the process is rather simple. Thus the flame fusion method is considered to be an adequate means for the synthesis of spherical particles. It is also expected that spherical particles of metal oxides can be prepared from metals in the oxidizing circumstance by this method. In fact, mill scale was treated in the propane-oxygen flame and completely oxidized spherical particles were obtained [6]. The objective of the present investigation was to establish the fabrication method of spherical magnetite particles with several tens μm diameter suitable for the magnetic carrier of PPC. In order to achieve this aim, iron powders with different sizes were oxidized and fused in the propane-oxygen flames using various propane/oxygen ratios and two experimental setups, and spherical particles obtained were characterized by various measurements.

0022–2461

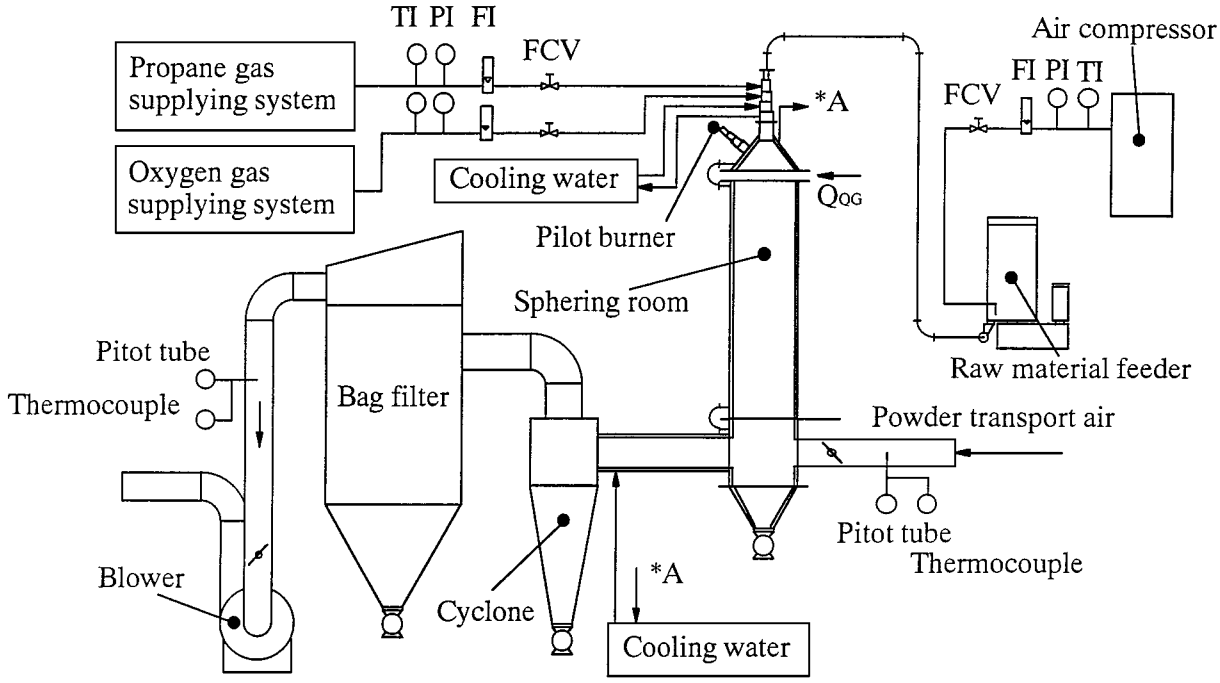

Figure 1 Experimental apparatus for fabrication of spherical magnetite particles. TI, PI, FI, FCV mean temperature indicator, pressure indicator, flow rate indicator and flow control valve respectively.

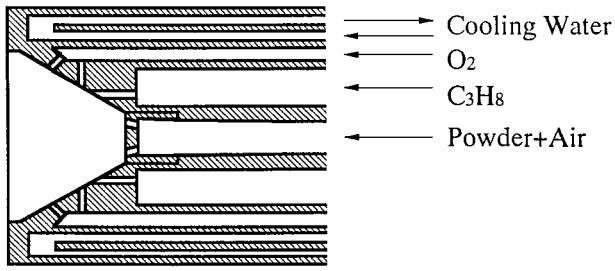

Figure 2 Schematic diagram of the burner.

2. Experimental

The experimental apparatus used in the study is shown in Fig. 1. Propane and oxygen were introduced into a burner nozzle illustrated in Fig. 2, of which details were described elsewhere [4, 5]. Ignition was carried out by a pilot burner flame. The flow rates of propane (Q_{LPG}) and oxygen (Q_{O_2}) were varied from 1 to 2 and from 2 to 20 Nm^3/h, respectively. Sponge iron powders with mean particle size of 35, 55 and 75 μm were used as starting powders and fed by a pneumatic table feeder using air as a carrier gas. The feed rate of iron powder (Q_{Fe}) was ranged from 20 to 40 kg/h and the flow rate of carrier gas (Q_{AIR}) was from 7.5 to 12.5 Nm^3/h. The mixture of iron powder and carrier air was introduced axially to a flame from the center of the nozzle and then into a sphering room (340 mm in diameter and 2000 mm in length) of which wall was cooled by water. The powder was cooled down there and collected by a cyclone and a bag filter with the aid of powder transport air which was introduced perpendicular to the sphering room at its lower part. In order to suppress the propagation of oxidation quenching gas (air) was injected. The quenching air injection flange was placed at the top extremity of the sphering room. The effect of quenching air was investigated with the flow rate of quenching air (Q_{QG}) from 0 to 18×10^2 Nm^3/h, which was calculated from flow rates of overall total gas, powder transport air, propane, oxygen and carrier air, and iron powder feed rate. The flame temperature was thermodynamically calculated from constituent gaseous species at the various points in the flame which was analyzed without feed of iron powder. Therefore the calculated temperature did not indicate the real flame temperature in the run, but was considered to give a good estimation concerning the temperature distribution in the flame. To observe the morphological change and progress of oxidation, particles in the flame were collected by a water-cooled probe which moved along the center line of the burner and sucked particles at various distances from the nozzle.

X-ray powder diffraction (XRD) patterns were obtained with (Ni-filtered) CuK_α radiation on a powder diffractometer (XD-3A, Shimazu Co., Ltd.) and used for identification of produced iron oxides and their amounts. The amounts of iron oxides and residual Fe in the products were evaluated from the ratio of intensities of a pure substance as standard and the corresponding one in the products. The reflections of 110 for Fe at $2\theta = 44.67°$, 200 for FeO at $2\theta = 41.93°$, 311 for Fe_3O_4 at $2\theta = 35.42°$ and 104 for α-Fe_2O_3 at $2\theta = 33.28°$ were chosen to calculate the content of each substance. Commercially available reagents were used as standard substances, Fe (iron metal, > 99.5%, Soekawa Chemicals), FeO (iron(II)oxide, 99.9%, Kojundo Chemical Laboratory), Fe_3O_4 (iron oxide, > 95.0%, Kanto Chemical), Fe_2O_3 (iron(III)oxide, > 99%, Merck). Special care was paid on the intensity measurement for the good reproducibility. The particle morphology was observed by scanning electron microscope (SEM, ABT-55, Akashi Beam Technology), while particle size distribution was determined by laser diffraction method

(Microtrac 7995-10PC SRA, Nikkiso Co., Ltd.). The saturation magnetization was measured by B-H curve tracer (BHU-60, Riken Denshi).

3. Results and discussion

Major part of products was collected in the cyclone and only small amount of very fine particles (about 3%) in the bag filter. Therefore we will discuss on powders collected in the cyclone, unless otherwise specified. As seen in Fig. 3, extensive morphological change was observed after the treatment in the propane-oxygen flame; irregularly shaped porous particles were turned to dense spherical particles. The spherical shape suggested that particles underwent fusion in the flame. XRD pattern showed that Fe, FeO, Fe_3O_4 and α-Fe_2O_3 existed in the products and their relative amounts were changed with the preparation conditions.

Fig. 4a and b indicates the change in content of oxides with Q_{O_2} at $Q_{LPG} = 1$ and 2, and $Q_{AIR} = 7.5\,Nm^3/h$. Iron powder with mean diameter of 35μm were fed and quenching air was not injected. Q_{Fe} was 32.1 kg/h when $Q_{LPG} = 1$ and 31.2 kg/h when $Q_{LPG} = 2$, respectively. The amount of Fe_3O_4 increased with Q_{O_2} but seemed to have a maximum of about 80% at Q_{O_2} of about 10 Nm^3/h in the case of $Q_{LPG} = 1\ Nm^3/h$ and about 13 Nm^3/h when $Q_{LPG} = 2\ Nm^3/h$. The amounts of remaining Fe and FeO decreased monotonously, while that of α-Fe_2O_3 increased with oxygen content in the system. Fig. 4 also shows that the atmosphere at $Q_{LPG} = 2$ is less oxidizing than at $Q_{LPG} = 1\,Nm^3/h$, as indicated by the less amount of Fe_3O_4 and the more Fe and FeO

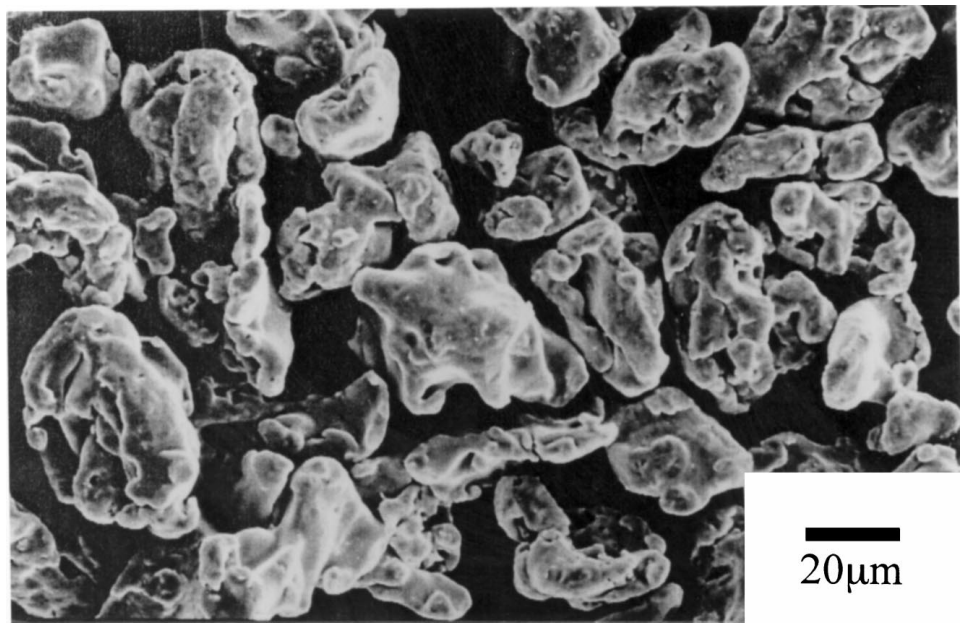

(a)

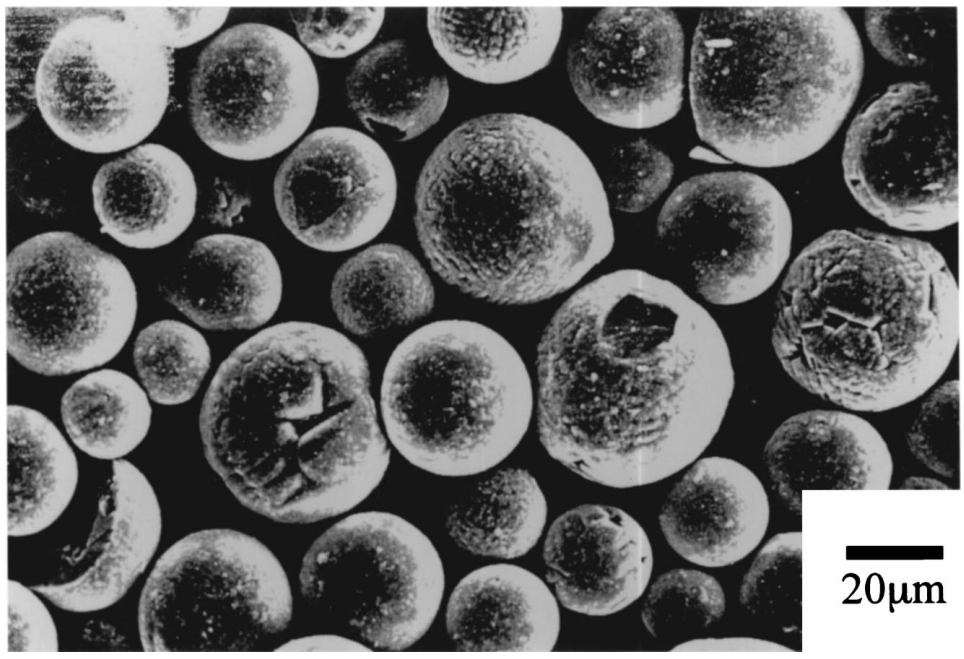

(b)

Figure 3 SEM photographs of (a) the starting powder and (b) microspheres of iron oxide collected by the cyclone. The powder was prepared at $Q_{Fe} = 1.0$ kg/h, $Q_{AIR} = 7.5\ Nm^3/h$, $Q_{LPG} = 1.0\ Nm^3/h$ and $Q_{O_2} = 5.0\ Nm^3/h$ using the starting powder with mean diameter of 35 μm.

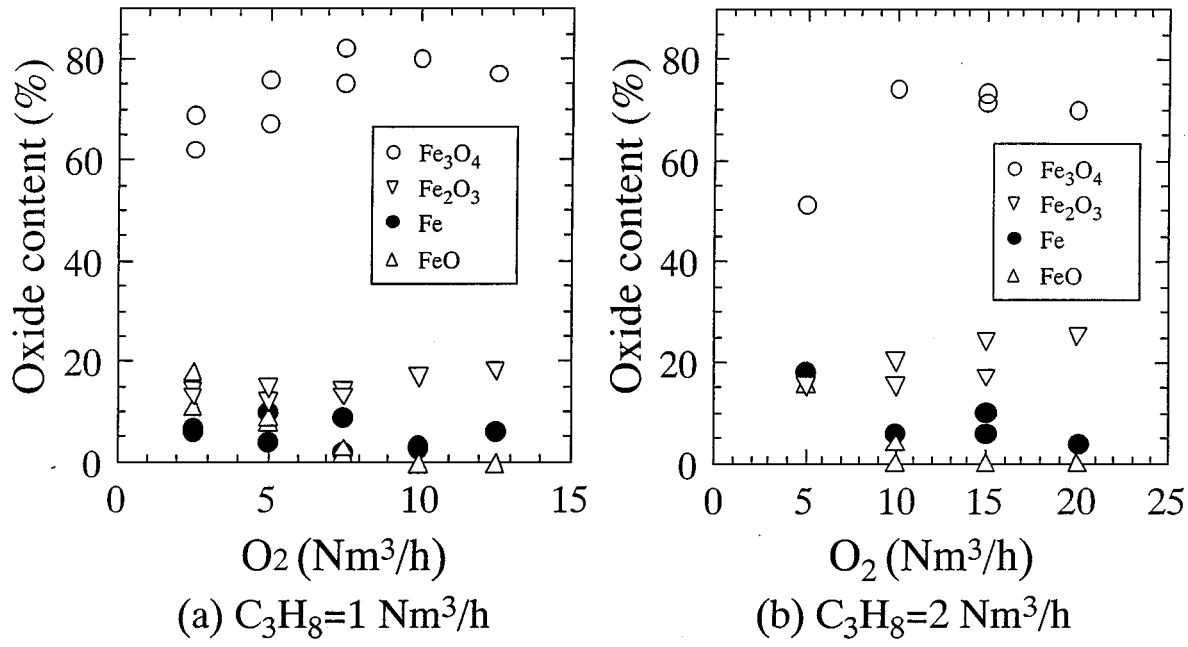

Figure 4 Relation between the content of oxides in the products prepared without quenching air and the oxygen flow rate at the propane flow rate of (a) 1 and (b) 2 Nm^3/h. Other experimental conditions were following: $Q_{Fe} = 32$ kg/h, $Q_{AIR} = 7.5$ Nm^3/h and the mean diameter of the starting powder was 35 μm.

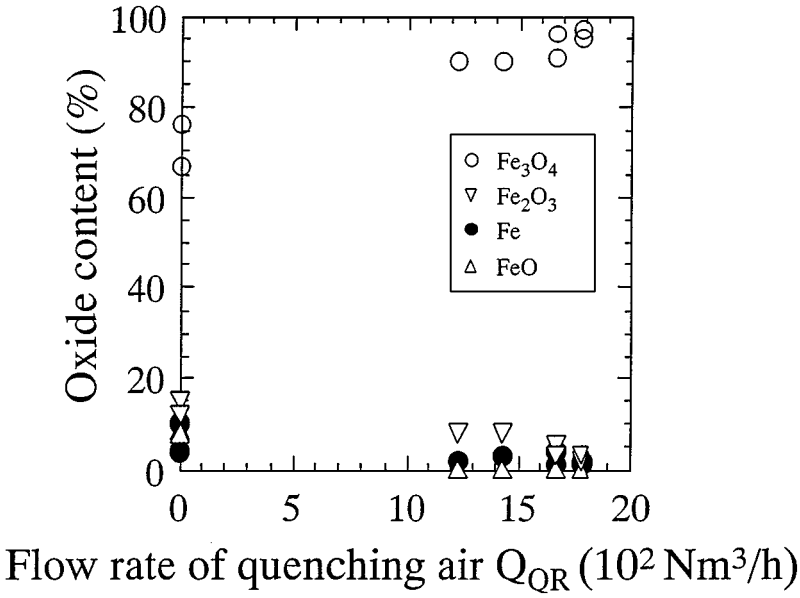

Figure 5 Change in the content of oxides with the flow rate of quenching air. The powders were prepared using the starting powder with mean diameter of 35 μm at $Q_{Fe} = 34$ kg/h, and $Q_{AIR} = 7.5$, $Q_{LPG} = 1$ and $Q_{O_2} = 5$ Nm^3/h, respectively.

amounts at $Q_{LPG} = 2\,Nm^3/h$ in the region of low flow rate of oxygen. The volume of oxygen which is necessary to oxidize completely 32.1 kg/h Fe to Fe_3O_4 and burn 1 Nm^3/h propane is calculated to be 13.6 Nm^3/h. Similarly, the amount of oxygen when $Q_{LPG} = 2$ Nm^3/h and $Q_{Fe} = 31.2$ kg/h is calculated to be 18.3 Nm^3/h. Taking the amount of oxygen in the carrier air (1.6 Nm^3/h) into account, the maximum amount of Fe_3O_4 was found to be obtained near the stoichiometric condition. The excess oxygen is considered to cause the oxidation of Fe_3O_4 to α-Fe_2O_3. In addition, produced Fe_3O_4 particles tends to be oxidized to α-Fe_2O_3 in contact with oxygen at high temperature. Therefore it is necessary to quench the further oxidation by cooling the particle temperature.

The effect of cooling is clearly seen in Fig. 5. A considerable increase of Fe_3O_4 up to 95% was obtained by introduction of quenching air of 1.7×10^3 Nm^3/h. As expected, suppression of oxidation from Fe_3O_4 to Fe_2O_3 was observed, especially at a high flow rate. At the same time, surprisingly, the amount of FeO was diminished, while Fe remained almost unchanged. According to the phase diagram of the system Fe-O given by Muan [7], FeO disproportionates to Fe and Fe_3O_4 below 843 K.

Therefore diminish of FeO might indicate that the residence time for the particles in the temperature range where the disproportionation reaction occurs was elongated by cooling. As the equipment of a large quenching system is not favorable from the industrial

point of view, the rate of quenching air was limited to about 1.8×10^3 Nm^3/h. The saturation magnetization of spherical Fe_3O_4 powder with a mean diameter of 36 μm which was prepared at Q_{LPG} of 1 Nm^3/h, Q_{O_2} of 5 Nm^3/h, Q_{Fe} of 35 kg/h, Q_{AIR} of 7.5 Nm^3/h and Q_{QG} of 1800 Nm^3/h was found to be 88 emu/g at room temperature. The formation of Fe_3O_4 particle was investigated with several variants as to feed rate of iron powder, flow rate of carrier air and mean particle diameter of iron powders at a constant quenching air rate.

As shown in Fig. 6, feed rate of iron powder did not considerably affect the amount of Fe_3O_4, although it seemed to decrease slightly at a high feed rate (>37 kg/h), accompanying a small increase of Fe. As the oxidation of iron itself evolves by the ignition of the heat of combustion, sphering and oxidation did not depend much on the feed rate of iron powder, as far as sufficient oxygen was supplied. On the other hand, as seen in Figs 7 and 8, rather large amount of iron

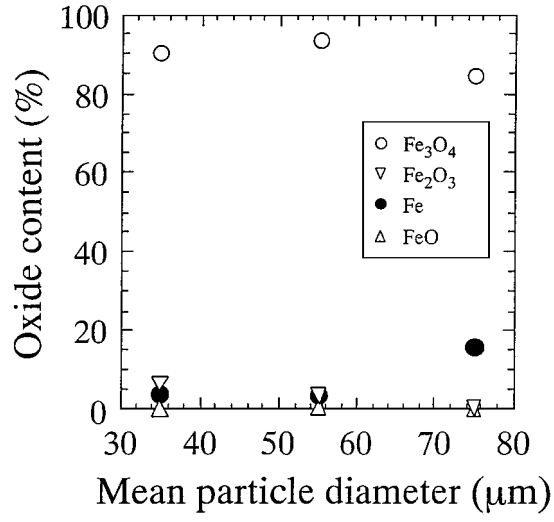

Figure 8 Change in the content of oxides with the mean diameter of the starting powder. The powders were prepared at $Q_{Fe} = 34$ kg/h, and $Q_{AIR} = 7.5$, $Q_{LPG} = 1$, $Q_{O_2} = 7.5$ and $Q_{QG} = 1782$ Nm^3/h, respectively.

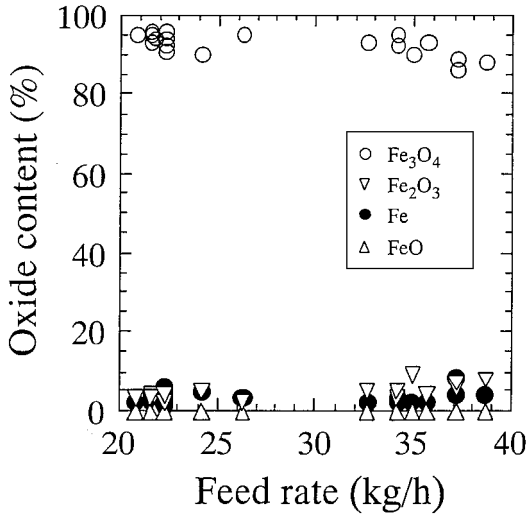

Figure 6 Change in the content of oxides with the feed rate of iron powder. The powders were prepared using the starting powder with mean diameter of 35 μm at $Q_{AIR} = 7.5$, $Q_{LPG} = 1$, $Q_{O_2} = 5$ and $Q_{QG} = 1782$ Nm^3/h, respectively.

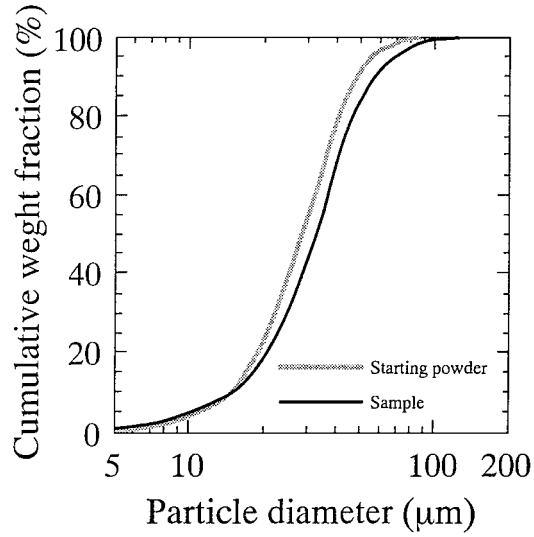

Figure 9 Particle size distribution of raw material (broken line) and cyclone-collected powder obtained at $Q_{Fe} = 34.2$ kg/h, and $Q_{AIR} = 7.5$, $Q_{LPG} = 1$, $Q_{O_2} = 5$ and $Q_{QG} = 1782$ Nm^3/h using the starting powder with mean diameter of 35 μm (solid line).

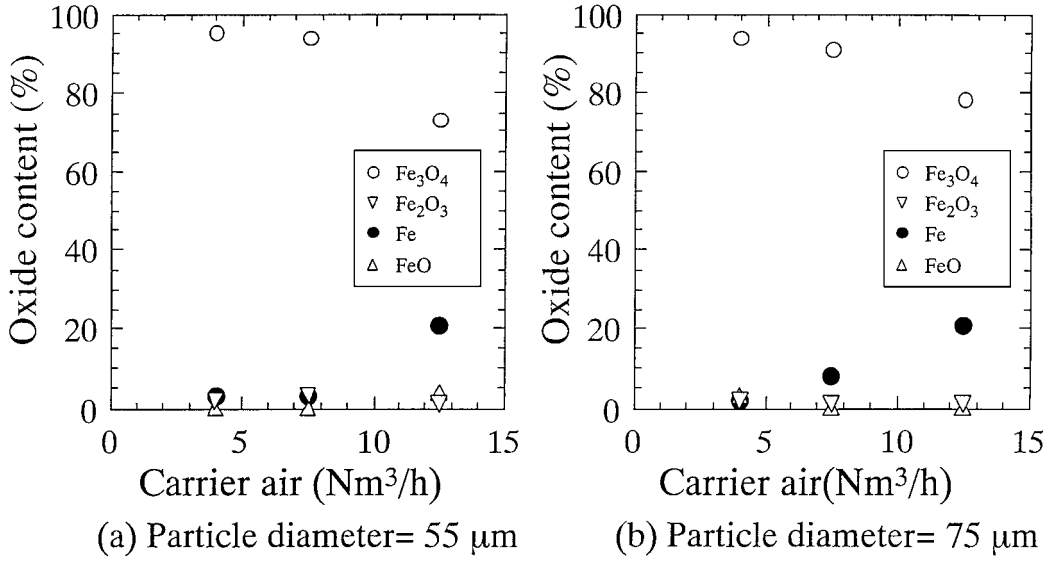

Figure 7 Change in the content of oxides with the flow rate of carrier air using the starting powder with mean diameter of (a) 55 and (b) 75 μm. The powders were prepared at $Q_{Fe} = 32$ kg/h, and $Q_{LPG} = 1$, $Q_{O_2} = 7.5$ and $Q_{QG} = 1782$ Nm^3/h, respectively.

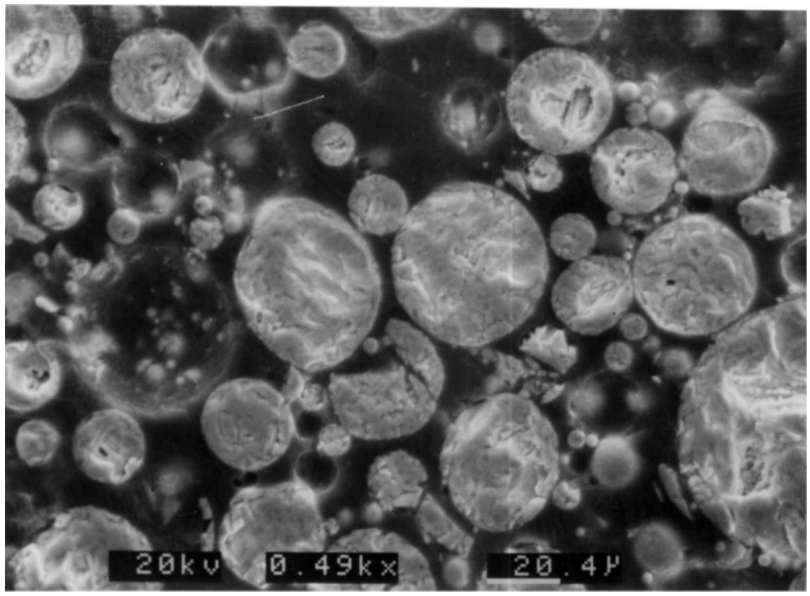

(a)

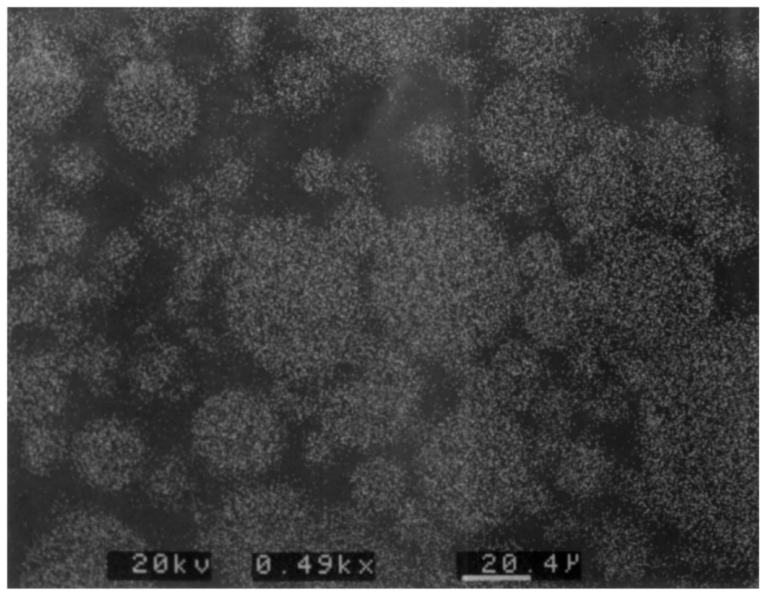

(b)

Figure 10 Section of typical spherical particles: (a) SEM photograph and (b) X-ray mapping of Fe.

was observed to remain unoxidized in the particle at a high flow rate of carrier air or using large particles. The high Q_{AIR} was considered to cause lowering of the flame temperature as well as acceleration of particles. Then the oxidation reaction was quenched in an insufficiently oxidized state. Similarly the residence time for the particles in the flame was not enough to oxidize completely a large particle.

The particle-size distribution of the starting powder with mean diameter of 31.06 μm and that of flame-fused and oxidized powder are shown in Fig. 9. The most populated size band of the product was located almost the same region of that of the starting powder, as if pores in the sponge iron were filled by Fe_3O_4 of which volume expands by about two times on the oxidation from 3Fe. This fact indicates that the control of particle size is much easier by this method than by the precipitation methods. The SEM photographs of sections of spherical particles in the powder containing $>95\%$ Fe_3O_4 revealed that each particle was composed of agglomerates of small crystallites and was not hollow as shown in Fig. 10. Because the distribution of FeK_α was homogeneous over the section as shown in Fig. 10, there is no evidence of segregated metallic Fe grains with the size observable by X-ray mapping. Even in the case of less oxidized particle the oxide shell and iron core were not observed. Table I shows the change of constituents and shape of particles in the flame with the distance from the nozzle. The oxidation seemed to proceed stepwise from Fe to FeO and from FeO to Fe_3O_4. Their regular shape of the starting powder was kept near the nozzle where the calculated temperature of 1174 K was below the melting point of iron and Fe was not oxidized. As the amount of oxides increased, partially fused particles were seen. When the volume of oxides became $>50\%$ at the calculated temperature

TABLE I Development of oxidation and morphology of particle in the flame

Distance[a] (mm)	Fe (wt %)	FeO (wt %)	Fe_3O_4 (wt %)	Fe_2O_3 (wt %)	Temp.$^{b}_{calc.}$ (K)	Morphology
50	100	0	0	0	1174	Irregular, same as the stating powder
100	89	10	1	0	2060	Fusion at limited parts
200	85	12	3	0	1433	Rounding of particles, very small number of spherical particles
300	62	33	5	0	2220	Increase of spherical particles
400	51	35	14	0	1099	Prevalence of spherical particles

[a]Distance from the top of nozzle.
[b]Temperature calculated from gaseous species in the flame without feed of iron powder.

of 1099 K, the number of spherical particles increased abruptly. Taking these facts and the phase diagram of Fe-O system into account, we can conclude that the liquid in the particle was oxide and metallic iron was dispersed in the liquid. The liquid phase made it easy for oxygen to diffuse into the particle and dispersed iron grains were oxidized ready. As the oxidation proceeds further, Fe_3O_4 might crystallize from the liquid in accordance with the phase diagram. Finally the liquid was solidified on cooling as Fe_3O_4 and FeO which disproportionated subsequently to Fe_3O_4 and Fe below 843 K. It turns out that the use of sponge iron as the

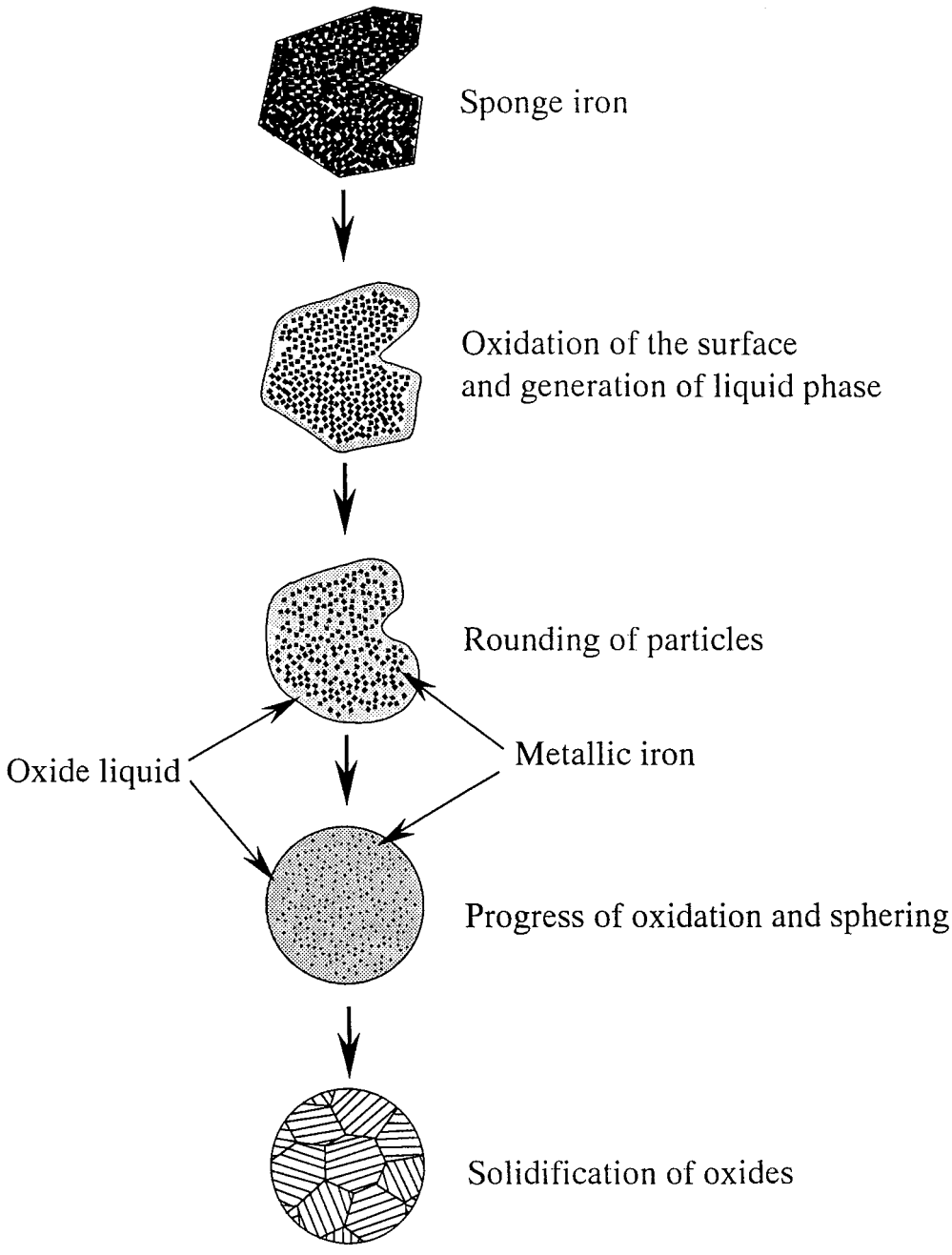

Figure 11 The process of spherical Fe_3O_4 particle formation.

starting powder is of great advantage to easy and overspreading oxidation of iron surface at the initial stage and the homogeneous dispersion of iron grains in the oxide liquid. The process of spherical Fe_3O_4 particle formation is illustrated in Fig. 11.

The fine particles collected by the bag filter were spherical particles with diameter of about 100 nm. The filter-collected powders were dark brown in color and were found to be almost composed of γ-Fe_2O_3 from XRD and TG measurements. The BET specific surface area of the powder was 19.2 m^2/g, coincided almost with the calculated one for γ-Fe_2O_3 powder with a particle diameter of 100 nm (11.5 m^2/g). This fact indicated that the particles were nonporous. It is well known that γ-Fe_2O_3 can be prepared from Fe_3O_4 by oxidation at low temperature ($<$673 K). But careful heat treatment and moisture were claimed to be essential for the reaction [8]. On the other hand, fine γ-Fe_2O_3 particles crystallized from gaseous phase in an oxygen-hydrogen flame and a low temperature plasma [9,10]. The stabilization of the metastable phase for massive materials was attributed to the change of surface characteristics with particle size. The evaporation and condensation mechanism accompanying oxidation of the injected iron powders is most plausible for the formation of such fine γ-Fe_2O_3 particles.

4. Conclusion

The saturation magnetization of spherical Fe_3O_4 powder with a mean diameter of 36 μm which was prepared at Q_{LPG} of 1 Nm^3/h, Q_{O_2} of 5 Nm^3/h, Q_{Fe} of 35 kg/h, Q_{AIR} of 7.5 Nm^3/h and Q_{QG} of 1800 Nm^3/h was found to be 88 emu/g at room temperature and the powder provided proper characteristics as a magnetic carrier for PPC. The oxidation of Fe_3O_4 to α-Fe_2O_3 was effectively suppressed by injection of quenching air and the yield of Fe_3O_4 was increased. As the particle size of products depends directly on that of starting powders, the fusion-oxidation method in the propane-oxygen flame enables easy control of particle size. It is interesting to point out that fine γ-Fe_2O_3 particles was synthesized from the vapor phase as a minor product.

References

1. The Society of Electrophotography, "Electrophotography—Bases and Applications" (Corona Publishing Co., Ltd., 1988) p. 481.
2. Japan Pat. 60-45262, 2-223962, 7-101731.
3. T. TODA, K. FUJIOKA, M. MIZUUCHI, K. MURASHIGE and K. TOGAWA, *J. Chem. Eng. Jpn.* **58** (1994) 446.
4. S. MIYAKE, T. SUZUKI and T. SUWA, *Inorganic Materials* **3** (1996) 219.
5. S. MIYAKE, N. KINOMURA, T. SUZUKI and T. SUWA, *ibid*. **4** (1997) 139.
6. K. ASANO, A. ISHII, M. MATSUO and J. YAMADA, in Proceedings of Annual Meeting of the Ceramic Society of Japan, May 1991, p. 544.
7. ARNULF MUAN, *Amer. Ceram. Soc. Bull.* **37** (1958) 81.
8. V. RAO, A. L. SHASHIMOHAN and A. B. BISWAS, *J. Mater. Sci.* **9** (1974) 430.
9. M. BOUDEULLE, H. BATIS-LANDOULSI, C. H. LECLERCQ and P. VERGNON, *J. Solid State Chem.* **48** (1983) 21.
10. G. P. VISSOKOV, *J. Mater. Sci.* **27** (1992) 5561.

Received 18 August 1997
and accepted 15 December 1998